

Final Report, 2023-2024 Funding Cycle
California Grape Rootstock Improvement Commission
California Grape Rootstock Research Foundation
American Vineyard Foundation

Luis Diaz-Garcia

Assistant Professor
Department of Viticulture and Enology
University of California, Davis

Project title: Foundations for a Modern Breeding Program

1. Summary

This project focuses on current efforts to modernize the grape breeding program at UC Davis, with an emphasis on two key areas: A) **tool development** and B) **data management**. In terms of tool development, our efforts are directed towards creating high-throughput phenotyping methods to evaluate A1) **chloride exclusion**, A2) **boron exclusion**, A3) **plant growth**, and A4) **root architecture**.

A1) **Chloride exclusion** is an important trait that allows certain genotypes to avoid chloride uptake in high-salinity soils. A2) **Boron exclusion** operates similarly but is a less-studied field, both in terms of exclusion mechanisms and boron sensitivity across commercial rootstocks and wild germplasm. Current screening methods for these two traits are time-consuming, which limits the number of plants that can be assessed. To address this, we have developed a novel methodology based on hyperspectral proximal sensing, allowing for the non-destructive and rapid prediction of chloride and boron exclusion capabilities. For A3) **plant growth**, we have designed a robotic platform equipped with imaging sensors to capture daily images of plantlets under water stress. We hypothesize that drought-tolerant genotypes will exhibit higher growth rates, making this tool useful for early-stage filtering of susceptible genotypes. The hardware is fully functional, and we are finalizing the software for image processing and analysis. A4) **Root architecture** is another critical trait linked to drought tolerance. Drought-tolerant rootstocks typically exhibit steeper root angles, thicker roots for deep soil penetration, and root growth that responds dynamically to soil moisture. These traits help focus root growth in deeper, wetter soil layers, enable rapid root regeneration after drought, and facilitate water uptake. To study root architecture, we have developed a low-cost protocol involving the use of minirhizotrons for plant growth and root visualization, coupled with AI-powered computer vision to extract root architecture features with high temporal and spatial resolution.

In B) **data management**, we developed a new database specifically for the UC Davis grape breeding program. This is essential due to the massive volume of data generated by the tools discussed above and the genotypic data being collected. The database will store phenotypic (RGB and hyperspectral images, traditional records, hyperspectral profiles, etc.) and genotypic data (rhAmpSeq markers, WGS, GBS, etc.), metadata (passport information, pedigrees, presence/absence of relevant alleles, etc.), as well as relevant breeding program actions such as crosses, propagation events, or trials. This will improve program efficiency, allow for tracking genetic gain over time, prevent data loss, and secure sensitive information.

The results from this project have been published in one peer-reviewed article and presented to industry groups (n=9) and at scientific meetings (n=2). At least two additional articles based on results from this project are currently in preparation and will be submitted for review in the first quarter of 2025.

2. Annual or Final Report: Final Report

3. Project title and UGMVE proposal number: Foundations for a Modern Breeding Program. #2023-2781

4. Principal Investigator/Cooperator(s):

Principal Investigator: Luis Diaz-Garcia, Dept. Viticulture and Enology, UC Davis. One Shields Ave, Davis, CA 95616-2027. tel: 530-754-2985, email: diazgarcia@ucdavis.edu
Cooperators: Dario Cantu & Megan Bartlett, Dept. Viticulture and Enology, UC Davis.
Andrew McElrone, USDA – ARS and Viticulture and Enology, UC Davis

5. Objectives and Experiments conducted to meet objectives

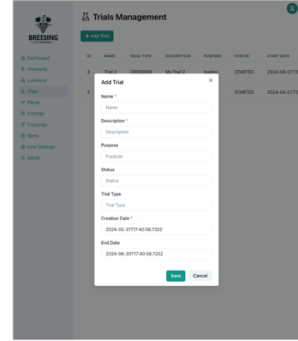
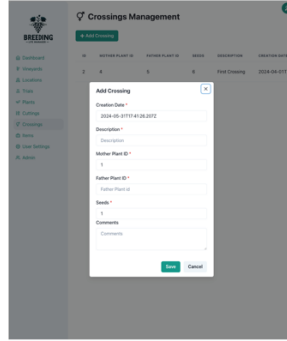
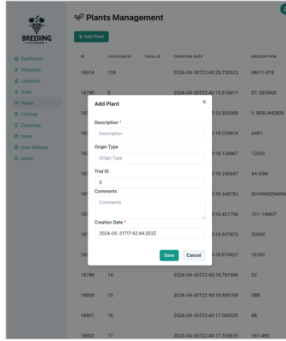
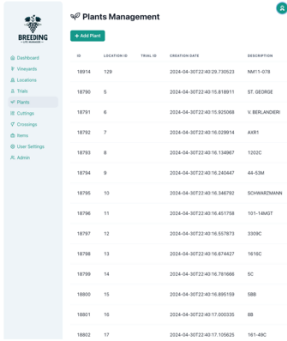
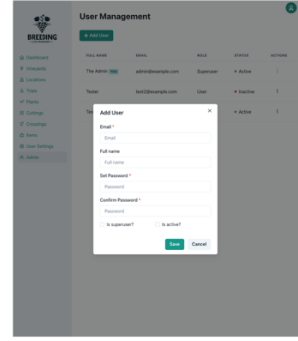
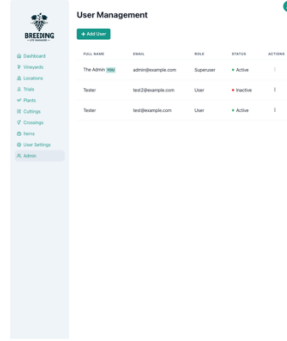
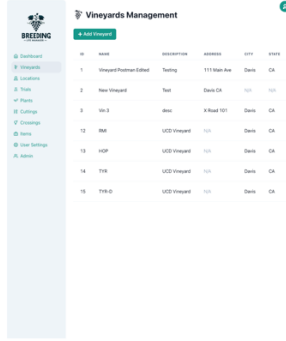
Objective 1. Build a comprehensive digital infrastructure for breeding data management

Several commercial and free software solutions, such as Breedbase and Germinate, are available to store and manage breeding information. However, these databases often present challenges due to their complexity and the difficulty of adapting their rules and operations to grape breeding. For example, grape breeders work with grafted vines, which involve the union of two different genotypes. Most available databases struggle to accurately represent grafted vines. Additionally, grapevines can originate from seeds or through dormant/hardwood or green cuttings, and maintaining this information is crucial for decision-making later in the breeding process. Representing these different plant origins efficiently in existing databases is also problematic. Furthermore, the learning curve for these systems is notably steep.

Therefore, we have decided to create a completely new database tailored to the specific needs of our grape breeding program while adhering to data management best practices and conventions (Figure 1A). To enhance the system's design and functionality, we are applying Domain-Driven Design (DDD) principles. This approach allows us to focus on the core domain of grape breeding and ensure the software accurately reflects the breeding processes' complexities. By collaborating closely with domain experts, we can model the system based on real-world scenarios, leading to a more intuitive and effective solution that aligns with the actual needs and workflows of the breeding program. Employing DDD also enables us to create a flexible and scalable architecture that adapts to our breeding program's evolving requirements. Using bounded contexts, we can manage different aspects of the system independently, reducing complexity and improving maintainability. For instance, separate contexts for vine propagation, inventory management, and trial administration allow for targeted and efficient development. This modular approach facilitates better integration with other systems and ensures that changes in one part of the system do not negatively impact other components. Additionally, we are developing dedicated workflows that align with physical actions in the program, including (but not limited to) the comprehensive management of trials and associated materials like cuttings, crossings, seeds, plants, and locations. This ensures that breeders and collaborators can efficiently execute and manage experiments. We are currently working on incorporating capabilities for storing high-dimensional phenotypic and genotypic data, such as RGB and hyperspectral images, single-point spectral profiles, manually recorded traits, and molecular markers.

The system's frontend is developed using React, providing a dynamic and responsive user interface (see Figure 1B). The backend exposes an API written in Python using FastAPI, ensuring efficient and high-performance communication between the frontend and the database. The database is built in PostgreSQL, interfaced and abstracted using SQLAlchemy, with Alembic handling database migrations. Both the frontend and backend can be deployed independently as dockerized containers, allowing for flexible and scalable deployment options.

A



B

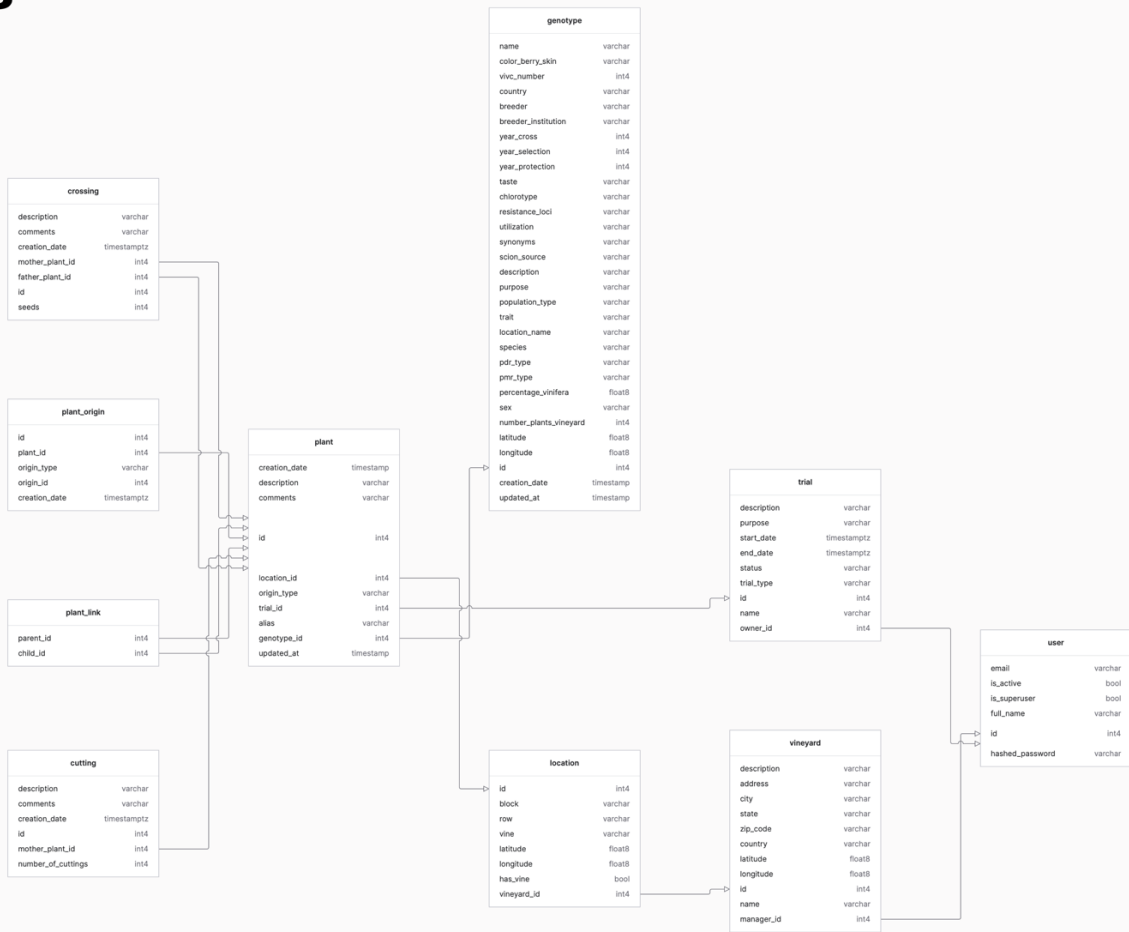


Figure 1: Custom Database System for Grape Breeding Program. (A) User interface screenshots: The custom-built database system tailored for the grape breeding program. The interface incorporates various management modules, including: *Vineyard Management*: handles information about different vineyard plots. *User Management*: manages user roles and permissions. *Plant Management*: allows for the input and tracking of plant information. *Crossing Management*: facilitates the recording and tracking of plant crossings. *Trial Management*: manages trial experiments and associated data. (B) Visual representation of how the various entities and their relationships are structured to support the specific needs of grape breeding, including crossings, pedigrees, plant inventories, vine locations, trials, metadata, and phenotypic and genotypic data, among others.

The 2025 season will be dedicated to field testing this new application. Currently, we are developing methods to identify individual vines in the vineyard using NFC tags (Figure 2), which operate on the same communication protocol as contactless payments. These tags, currently being tested on field vines, are connected to the database discussed above. This will streamline vine identification when collecting plant material for propagation, making crosses, or recording field data. Depending on their privileges defined in the database, users will have access to different levels of information by simply scanning a tag on a vine. This access can range from



viewing basic details, such as the row and column location, to more comprehensive information, including scion/rootstock names, pedigrees, passport data, and previously collected data.

We plan to tag all the vines in one of the largest blocks in the collection (~2,500 vines), which includes the majority of the Southwestern diversity collected by Walker. This collection contains most of the trait donors for drought, salt, and boron tolerance.

Figure 2. NFC tag for digital vine identification

Objective 2. Develop high-throughput methods for faster and more precise phenotyping.

This objective aims to develop high-throughput phenotyping techniques to screen for **chloride exclusion, plant growth, and root architecture**. The first technique will enable more efficient identification of salt-tolerant rootstocks, while the latter two are expected to provide valuable information for identifying traits indicative of drought tolerance. Recently, boron exclusion was also prioritized in the program, and similar work to that conducted for chloride exclusion is being carried out for this trait.

Chloride exclusion: We investigated the use of hyperspectral data for predicting chloride content in several *Vitis* species with potential for rootstock breeding. Two similar experiments were conducted as full factorial designs, with five repetitions per genotype:salt treatment combination. Salt treatments, initiated two months after transplanting, comprised three NaCl levels (0 mM, 50 mM, and 75 mM of NaCl) and lasted for 21 days. Each pot was watered with one liter of the respective saltwater concentration every morning between 7 and 8 AM. Both trials utilized the

same 23 accessions, experimental design, and treatments. The 23 accessions examined spanned 10 species, namely *V. cinerea*, *V. berlandieri*, *V. girdiana*, *V. acerifolia*, *V. treleasei*, *V. arizonica*, *V. mustangensis*, *V. × champinii*, *V. × doaniana*, and *V. rupestris*, along with two commercial rootstocks, 140 Ru and Ramsey. The accessions were selected based on previous chloride exclusion screenings (Heinitz et al., 2020).

We utilized hyperspectral information from two different instruments, the HR-1024i and the NIR-S-G1, which vary in price, resolution, and sensitivity. The HR-1024i (Spectra Vista Corporation in Poughkeepsie), coupled with a leaf clamp (LC-RP Pro), is a field-portable spectroradiometer that records reflectance spectra across wavelengths from 350 to 2500 nm. Its resolution varies: 1.5 nm between 350 and 1000 nm, 3.8 nm from 1000 to 1890 nm, and 2.5 nm from 1890 to 2500 nm. Despite its larger size, the HR-1024i remains portable. The other instrument, the NIR-S-G1 (Innospectra Corporation), captures reflectance within the 900 to 1700 nm range, with a spectral resolution of 3 to 4 nm. This device is remarkably smaller and costs approximately 20 times less than the HR-1024i.

Hyperspectral reflectance on leaves was validated with leaf chloride content determined using a lab chloridometer. Stomatal conductance (gs) and ϕ PS2 were also measured with a porometer/fluorometer to assess physiological stress responses. Hyperspectral reflectance and chloride content were used to develop prediction models using three approaches: 1) Analyzing the correlation between individual wavelengths and chloride content; 2) utilizing machine learning models, including partial least squares regression (PLSR), random forest (RF), and support vector machine (SVM), leveraging all wavelengths; and 3) classification-based prediction using Partial Least Squares Discriminant Analysis (PLSDA).

As expected, we observed no salt stress symptoms in the control plants (0 NaCl). Under salt stress, different responses were observed. For example, *doaniana* 9026 (*V. × doaniana*), a chloride excluder accession, did not show any symptoms and seemed green under 75 mM salt treatment (Figure 3A). Conversely, non-excluder accessions, under salt stress (50 mM and 75 mM of NaCl) showed wilting with reduced vigor (Figures 3B and C). One of the non-excluder accessions, NM11-085 (*V. treleasei*), showed increasing affectations as stress increased; wilting and necrosis were observed at 50 mM salt treatment (Figure 3B), whereas at 75 mM salt treatment, necrosis, wilting, and yellowish leaves were observed (Figure 3C). In general, the brownish-white discoloration started from the margin of the leaves and extended inwards, typical of salt stress.

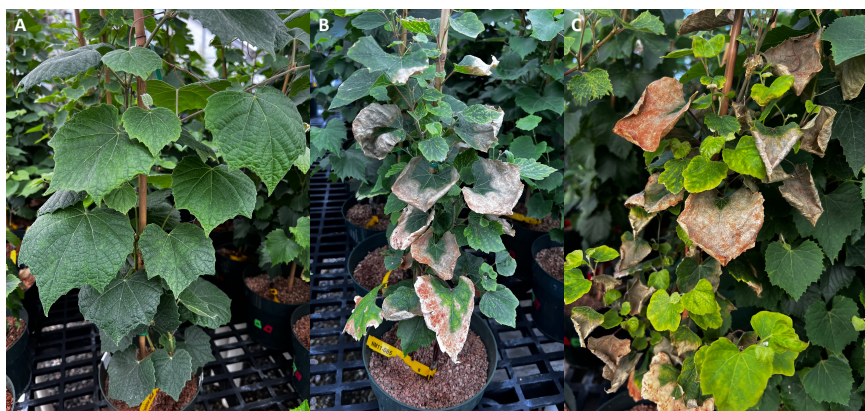


Figure 3. Symptoms of chloride toxicity in chloride-excluding and non-excluding accessions. (A) No symptoms of chloride toxicity observed on the leaves of accession *doaniana* 9026 (*V. × doaniana*) under 75 mM salt treatment. Wilting, scorching, and whitish brown discoloration on the

leaves of NM11-085 (*V. treleasei*) growing at (B) 50 mM and (C) 75 mM salt treatments.

Consistent results were observed across the two trials conducted. The chloride content in the first trial and second trial ranged from 0 to 7935.97 $\mu\text{mol}\cdot\text{g}^{-1}$ DW and 0 to 7945.27 $\mu\text{mol}\cdot\text{g}^{-1}$ DW, respectively. There was a high correlation (Pearson's $r = 0.93$) between trials 1 and 2 for chloride content (Figure 4A). Significant differences were observed in the treatment, accession, and the interaction between treatment and accession ($p\text{-value} < 0.0001$, one-way ANOVA) across both trials. Plants subjected to the 75 mM salt treatment had higher chloride accumulation in their leaves, followed by those treated with 50 mM, and then 0 mM. longii 9018, a *V. acerifolia* accession, was one of the best chloride excluders found in both trials, with 419.37 $\mu\text{mol}\cdot\text{g}^{-1}$ and 713.68 $\mu\text{mol}\cdot\text{g}^{-1}$ under the 50 mM and 75 mM treatments, respectively, confirming previous observations (Heinitz et al., 2020). longii 9018 performed comparably to 140Ru (a commercial rootstock derived from *V. rupestris* and *V. berlandieri*), doaniana 9024 (*V. \times doaniana*), doaniana 9026 (*V. \times doaniana*), girdiana SC (*V. girdiana*), and longii 9035 (*V. acerifolia*) at 50 mM (Dunnett's test, $p\text{-value} = 0.05$; Figure 4B). However, at 75 mM, the commercial rootstock 140Ru exhibited statistically significant higher chloride accumulation compared to longii 9018 and the aforementioned chloride excluder accessions, underscoring the importance of other species in acquiring adaptive traits for breeding.

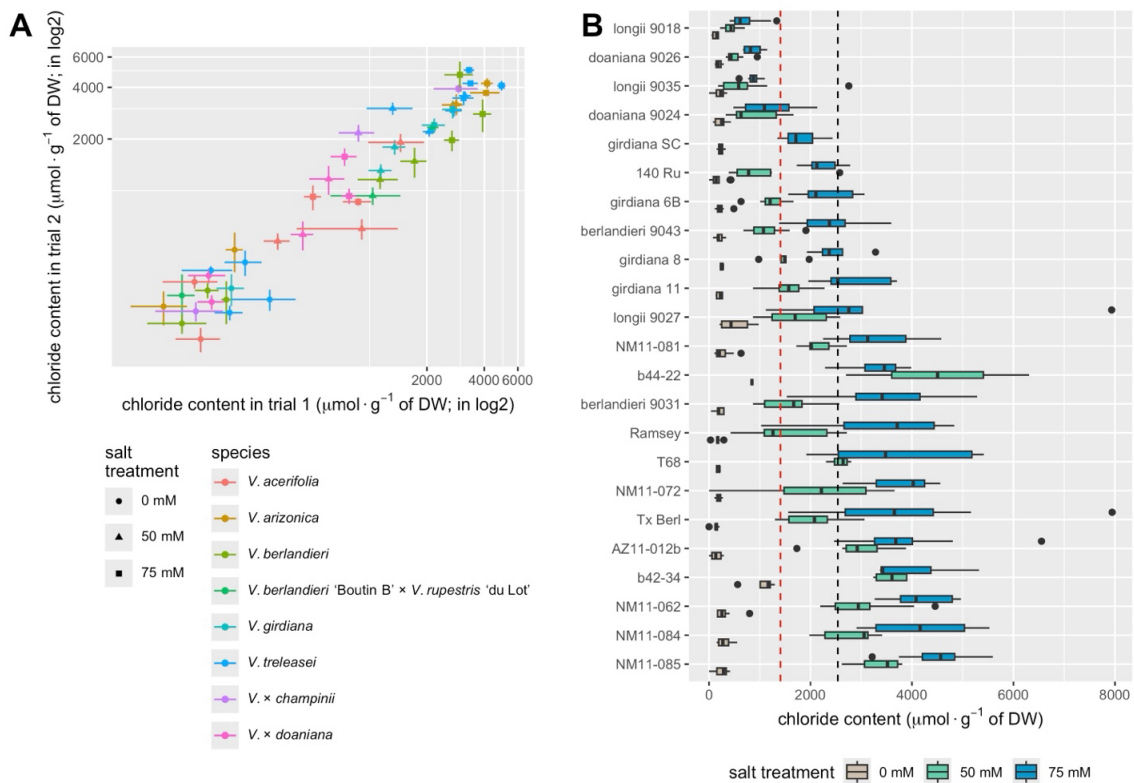


Figure 4. Variability in chloride content accumulation across *Vitis* germplasm. (A) Correlation between trials 1 and 2 for leaf chloride; lines represent standard errors for each accession within their corresponding trial. **(B)** Leaf chloride content for 23 accessions under three salt treatments (0, 50, and 75 mM of NaCl). The red dashed line corresponds to the threshold of 1410.44 $\mu\text{mol}\cdot\text{g}^{-1}$ DW, while the black dotted line represents the threshold of 2538.79 $\mu\text{mol}\cdot\text{g}^{-1}$ DW; these thresholds are used to classify excluders and non-excluders in the PLSDA approach..

Stomatal conductance (g_s) varied between 0.01 to 0.98 $\text{mol}\cdot\text{m}^{-2}\cdot\text{s}^{-1}$, with significant differences across varying salt treatments ($p < 0.001$, one-way ANOVA). Plants not subjected to salt stress (0 mM) exhibited the highest g_s , while no significant differences were detected between the 50 mM and 75 mM treatments (Figure 5A). ϕPS2 values ranged between 0.06 to 0.75 with significant differences among all treatment groups ($p < 0.001$, ANOVA test). ϕPS2 was significantly higher ($p < 0.001$, one-way ANOVA) in plants with no salt treatment (0 mM) and gradually decreased in plants treated with 50 mM and then 75 mM salt (Figure 5B). These observations demonstrated that the salinity treatments applied in these trials induced marked physiological stress, in addition to visible symptoms.

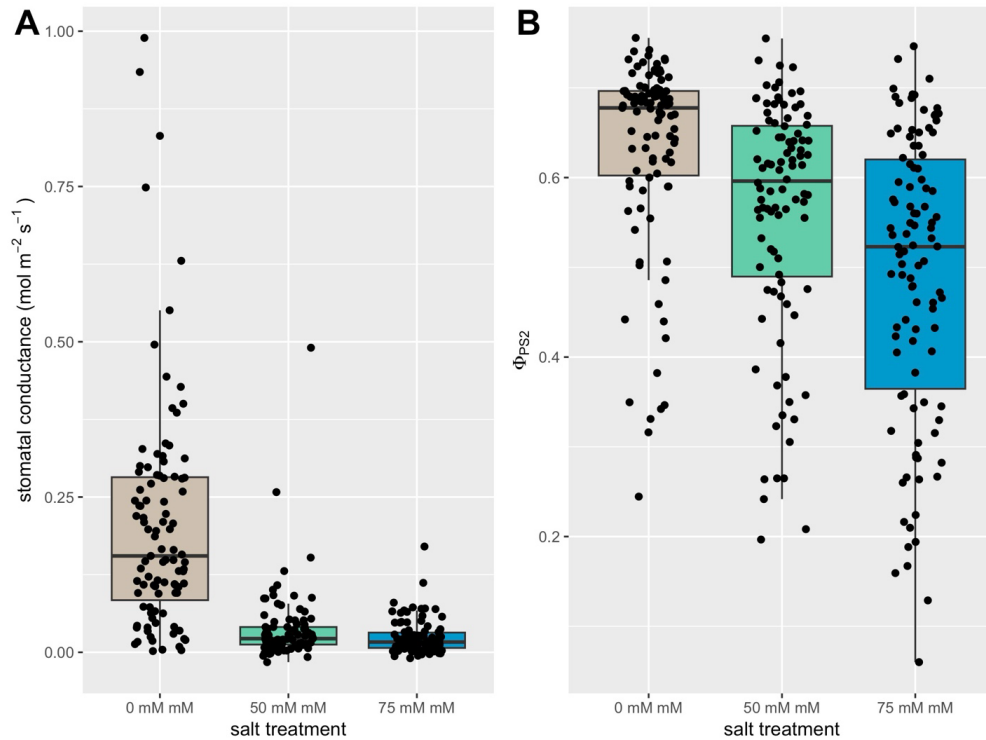


Figure 5: Impact of salt stress on physiological traits. (A) stomatal conductance (g_s), and **(B)** ϕPS2 under different salt stress treatments; in both panels, points correspond to individual plants.

Multiple regions in the spectrum, including 613-660 nm, 689-696 nm, and 1357-1358 nm, showed correlations (Pearson's r) of 0.30, 0.32, and 0.50 with chloride content in the leaf, respectively (Figure 6A). Additionally, PLSR predicted chloride content with moderate effectiveness (maximum $R^2 = 0.67$), although differences were noted between the two devices tested (Figure 6B). An improvement was observed in both devices when employing PLSDA, with prediction accuracies ranging from 0.69 to 0.97, depending on the instrument used and the treatment applied to the spectral data (Figure 6C).

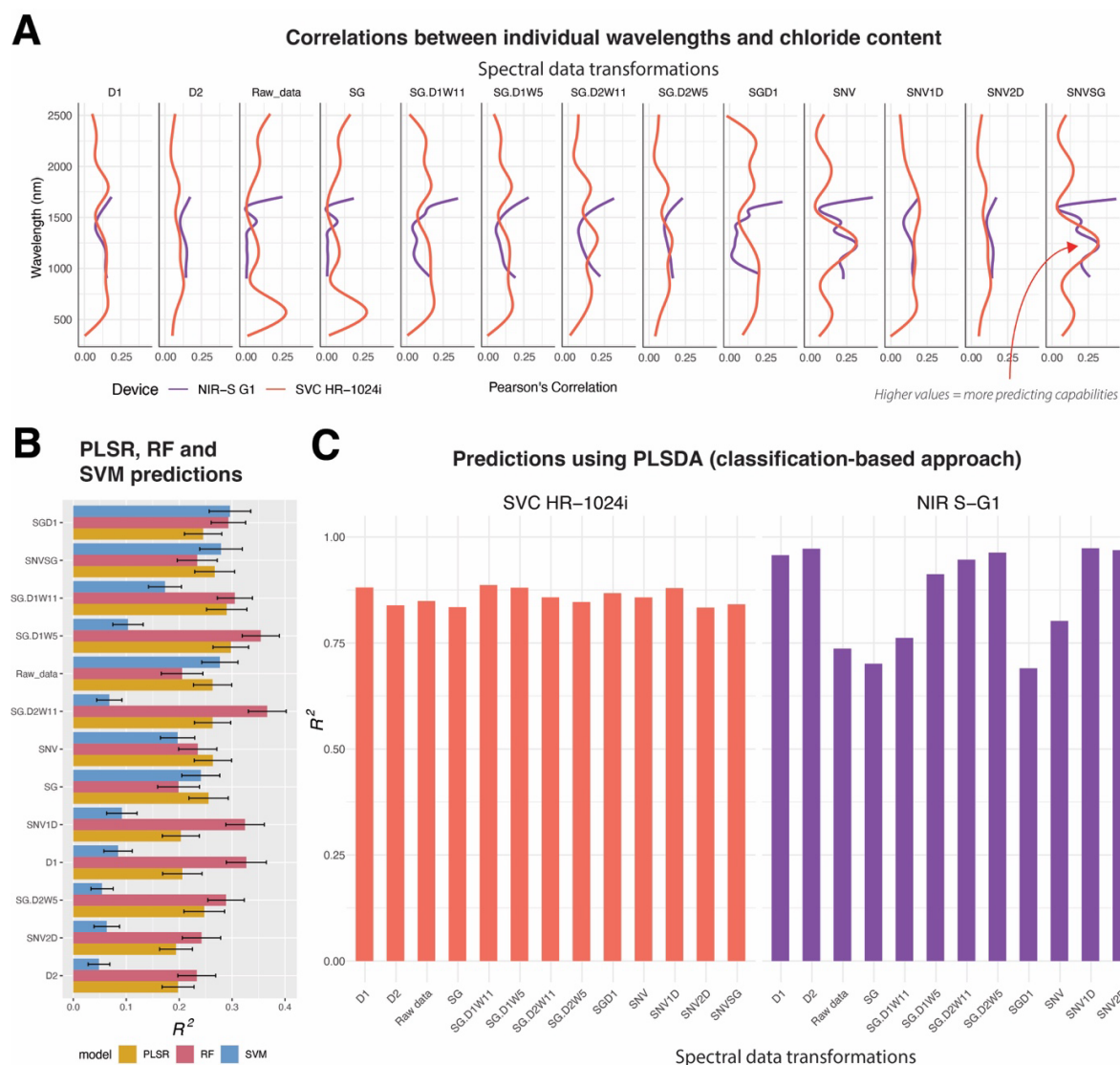


Figure 6. Prediction capabilities using different approaches. (A) Pearson's correlations between chloride content and reflectance at individual wavelengths recorded with the SVC HR-1024i (red) and NIR-S G1 (purple). Pearson's correlations for different pretreatments along with raw data are shown in different panels. Treatments include first derivative (D1), second derivative (D2), raw data, Savitzky-Golay filter (SG), Savitzky-Golay with window size = 11 and first derivative (SG.D1W11), Savitzky-Golay with window size = 5 and first derivative (SG.D1W5), Savitzky-Golay with window size = 11 and second derivative (SG.D2W11), Savitzky-Golay with window size = 5 and second derivative (SG.D2W5), gap segment derivative with window size = 11 (SGD1), standard normal variate (SNV), standard normal variate and first derivative (SNV1D), standard normal variate and second derivative (SNV2D), and standard normal variate and Savitzky-Golay filter (SNVSG). **(B)** Raw data along with 12 treatments applied to spectral data from NIR-S G1 shown in the Y-axis and squared Pearson's correlation between observed and predicted values in the test set (R^2) displayed in the X-axis. **(C)** Accuracy and specificity results for PLSDA with raw data and 12 treatments for both devices - SVC HR-1024i and NIR-S G1.

The capability to screen thousands of plants during the breeding process can increase genetic gain by allowing higher selection intensities. However, given that breeding program budgets are typically constrained, we must consider the cost-effectiveness of new screening methodologies relative to the expected improvement in genetic gain. The NIR-S G1 achieves comparably high accuracy (>0.90, depending on the spectral data transformation) when the objective is simplified to a classification problem (chloride excluder vs. non-excluder). Despite its relatively low price, this technique will enable the breeding program to significantly increase the volume of plants screened for chloride exclusion while keeping screening costs low, given the minimal investment in equipment.

Using this newly developed method, we are also screening a collection of *Vitis* germplasm of about 400 individuals. These individuals encompass more than 15 species, some of which have preliminary observations pointing to good exclusion capabilities and, therefore, potential for breeding salt-tolerant rootstocks. This germplasm collection has been genotyped previously by our collaborator Dario Cantu (Cooperator in this project), and about 20 million markers are available for each accession. The phenotypic (chloride exclusion) and genotypic data will be combined for conducting a genome-wide association analysis (GWAS) to identify genomic regions linked to the trait variation.

Boron exclusion: Boron plays a critical role in plant growth and development by contributing to cell wall structure, membrane functionality, and various metabolic processes. It influences calcium uptake, sugar translocation, pollen germination, hormone regulation, root development, and the formation of flowers and fruits. However, in regions like California's Central Valley, boron toxicity due to high soil concentrations poses a significant challenge. Toxicity symptoms, including leaf necrosis and oxidative stress, can impair vine growth and reduce yields. Environmental factors such as arid climates and saline soils exacerbate boron toxicity by limiting its leaching. As climate change pushes viticulture into new regions with varying soil conditions, understanding boron's dual role—as both a vital nutrient and a potential toxin—is crucial for developing resilient grapevine rootstocks and sustainable vineyard practices.

Unfortunately, no in-house protocol exists for screening boron tolerance in grapevines, such as the chloride screening method that uses a chloridometer. Instead, tissue analysis must be conducted in external labs at a cost of ~\$30–35 per sample. Additionally, there is little information regarding boron susceptibility across commercial rootstocks, whether under field or controlled greenhouse conditions. Similarly, sources of boron tolerance in wild *Vitis* species have not yet been identified, with only one or two accessions showing promise based on preliminary observations by Walker.

To address this, we conducted a large potted-vine trial using existing supplies. The trial included 16 genotypes, comprising commercial rootstocks and wild accessions, exposed to five boron concentrations: 0.5 ppm (control), 1 ppm, 2 ppm, 4 ppm, and 8 ppm. Each genotype-treatment combination included six plants, grown using the same protocol as chloride screenings. Weekly, the plants were measured with a CI-710 spectrometer to collect reflectance data in the 400–1100 nm range. At the end of the experiment, leaves from all plants were collected, and half were sent to a lab for tissue analysis to determine boron concentration.

Boron concentration in leaves after ~4 weeks of growth varied considerably across genotypes, ranging from ~200 mg/kg (GRN3) to >600 mg/kg (T03-15, a wild *V. rupestris* accession) at the highest boron stress level (8 ppm; Figure 7). Commercial rootstocks with

reduced boron accumulation included SO4, Schwarzmann, Riparia Gloire, and 110R. Higher boron accumulation was observed in 140Ru, 1103P, and 101-14. Several wild *Vitis* accessions, including longii 9018, longii 9035, and 2014-160-003, also showed low boron accumulation. As expected, at the lowest boron concentrations (0.5 ppm and 1 ppm), no significant differences were observed across genotypes.

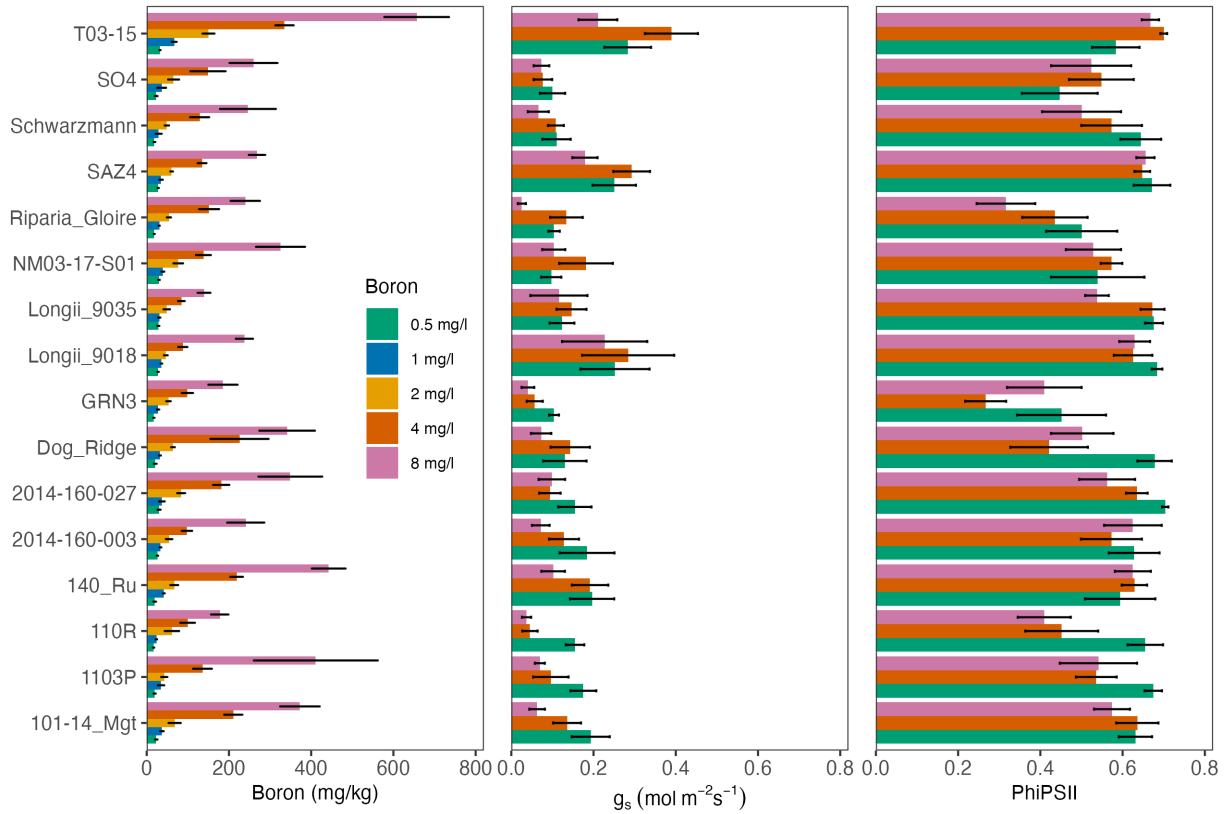


Figure 7. Boron accumulation in leaves, stomatal conductance, and Φ PS2 after 4 weeks of growth under different boron stress levels.

While these results revealed clear candidates for boron exclusion, they must be analyzed in the context of plant growth (as in Figure 8), as some exclusion mechanisms may not be compatible with commercial production (e.g., shutting down growth to prevent ion uptake). For instance, while GRN3 exhibited low boron accumulation in its leaves, its stomatal conductance and Φ PS2 values were lower than those of most other genotypes studied. This could indicate reduced gas exchange, a lower photosynthesis rate, and potentially limited growth.

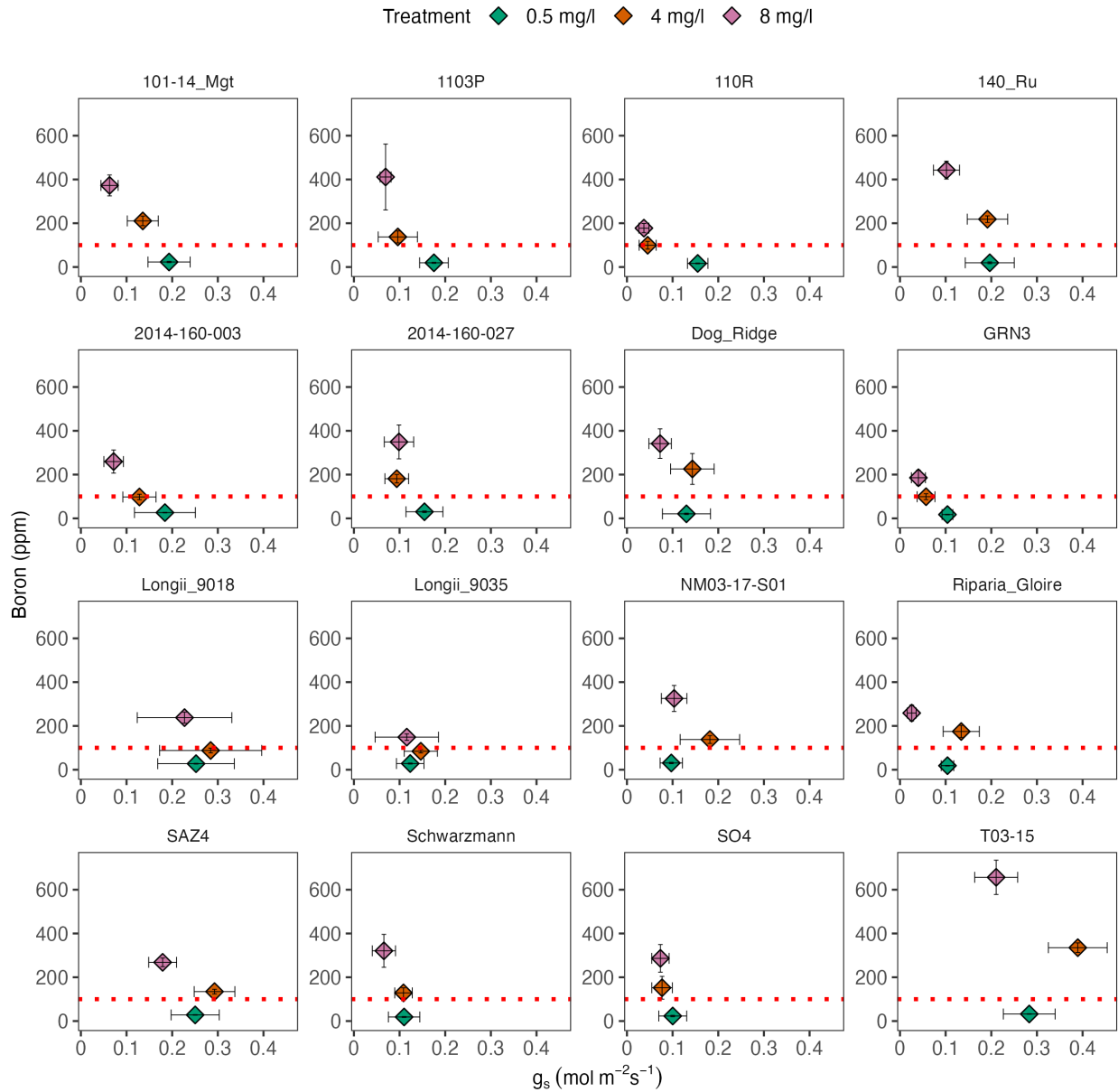


Figure 8. Relationship between boron leaf accumulation and stomatal conductance across genotypes. The red line indicates a reference value of 100 ppm.

Preliminary analysis of the spectral data shows a clear effect of boron stress levels on reflectance values, particularly in the 550–750 nm range (Figure 9). Currently, prediction models based on hyperspectral data are being developed using similar strategies to those used for chloride.

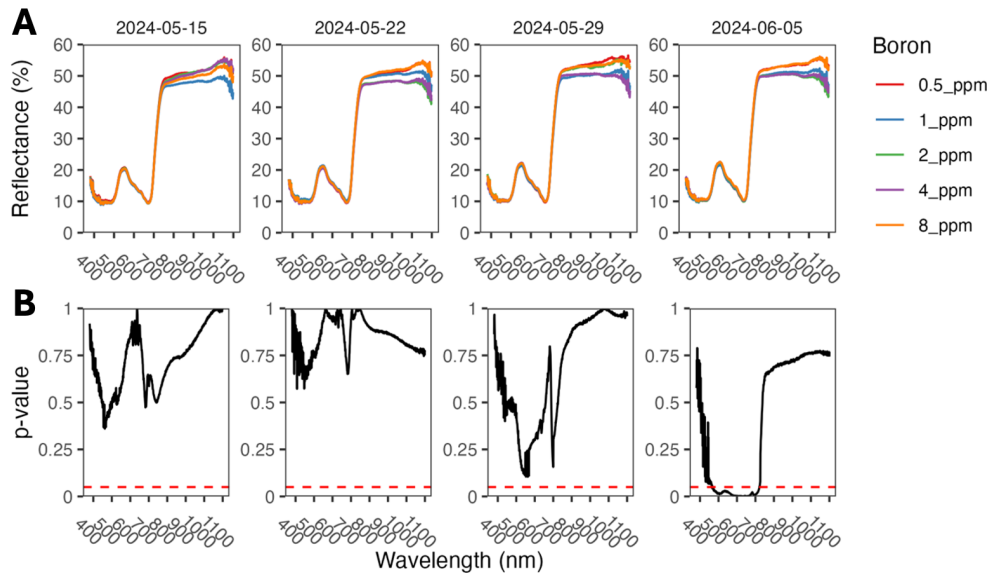


Figure 9. Preliminary analysis of spectral data under boron stress conditions. (A) Average spectral profiles across genotypes subjected to varying boron stress treatments. **(B)** Statistical significance of the slope from a model assessing reflectance as a function of boron stress level. Red line corresponds to $p\text{-value}=0.05$

Robotic platform for measuring plant growth: We hypothesize that drought-tolerant genotypes will exhibit higher growth rates under water stress conditions compared with susceptible genotypes. In this project, we are testing if recently propagated, young plantlets can be used to screen growth rates and infer drought tolerance levels. To do so, we have built a robotic platform called Phenobot for automating RGB and hyperspectral image acquisition (Figure 10). We propose that this robotic platform can be used to quantify small changes in growth rate parameters and hyperspectral reflectance for thousands of plants in water deficit/nutrient stress trials.

In its current form, the robot's structure consists of an aluminum frame and tracks spanning a coverage area of 30m². The gantry, or the structural column, connects the two tracks and moves along the y-axis. Additionally, the gantry acts as a guide, enabling the x-axis slide plate to traverse across it, utilizing a timing belt and pulley system akin to that of the y-axis. The lead-screw, threaded through a block attached to the x-axis slide plate, enables movement along the z-axis. NEMA stepper motors drive the Phenobot's movement along its tracks and also drives the z-axis leadscrew, facilitating precise positioning of both the camera and watering hose with mm-level accuracy. The Phenobot is equipped with a set of four 16MP RGB camera modules and Cubit Ultris 5 hyperspectral camera (450-850 nm). A Raspberry Pi oversees high-level operations, including communication via our prototype GUI, to maneuver the cameras and capture images. The robot was watering capabilities too. Depending on the size of the plants, the robot can accommodate up to 800, 1800, or 7200 plants growing in 6, 4, and 2-inch pots, respectively. Software-wise, we are developing an image processing algorithm capable of predicting biomass weight and plant height based solely on the four RGB images generated by the Phenobot. This estimation of biomass utilizes DepthAnything for monocular depth estimation and SegmentAnything.

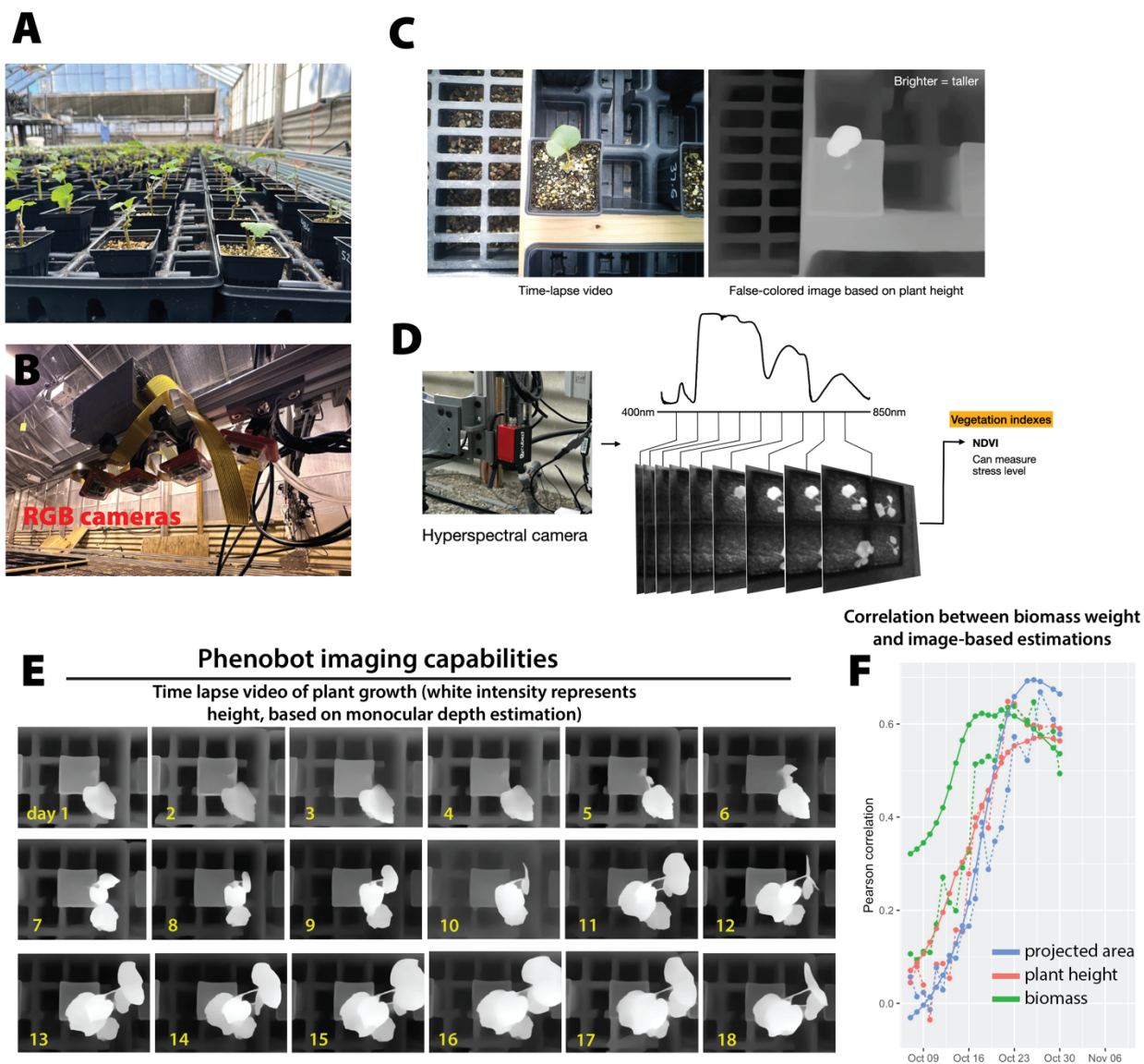


Figure 6. Robotic Platform for Measuring Plant Growth. (A) An image showing the initial setup of the plant growth trays inside a controlled environment greenhouse. Young plantlets are organized in individual pots to facilitate automated image acquisition. (B) Close-up view of the RGB camera setup on the Phenobot. Four 16MP RGB camera modules are mounted on the robotic platform for high-resolution image capture. (C) Workflow of the imaging process: (left) A time-lapse video of plant growth; (middle) RGB image captured by the Phenobot; (right) false-colored image representing plant height derived from monocular depth estimation. (D) The hyperspectral imaging setup on the Phenobot, equipped with a Cubit Ultris 5 hyperspectral camera (450-850 nm). The hyperspectral camera generates vegetation indices, such as NDVI, to measure plant stress levels. The inset shows a typical hyperspectral camera and the resulting spectral data across the visible to near-infrared spectrum. (E) Time-lapse sequence showing plant growth over 18 days, where white intensity in the images represents plant height, based on monocular depth estimation. This visualization demonstrates the Phenobot's capability to track growth dynamics accurately. (F) Correlation analysis between biomass weight and image-based estimations (projected area, plant height, and biomass).

The Phenobot system, along with its accompanying image-processing software, still requires further development and validation, which is something we will focus on the following months/years. For instance, we are currently testing a LiDAR sensor to generate 3D models of plants growing in the robot (Figure 11). This will allow the estimation of leaf area as well as a more reliable estimate of plant biomass.

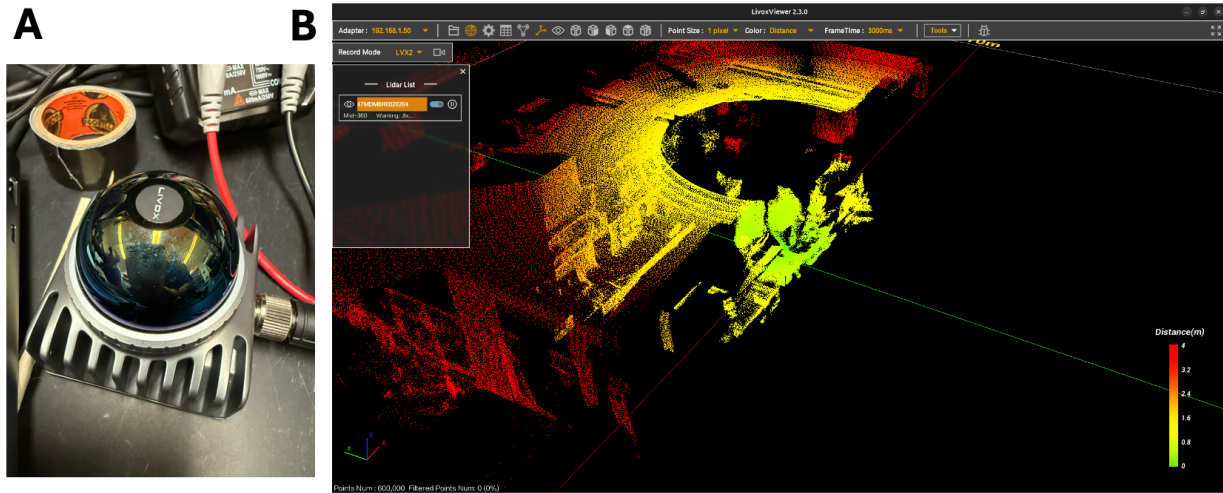


Figure 11. LiDAR sensor for 3D modelling. (A) LIVOX sensor. (B) Example of a point cloud obtained with the LIVOX sensor.

On the software front, improvements are being made to the GUI for more efficient robot control and data management. We are also focused on the analysis of hyperspectral images, a domain we have not yet fully explored. Specifically, we are investigating whether the algorithms applied to RGB images, especially those concerning depth estimation, can be adapted for plant segmentation purposes on hyperspectral images. Subsequently, we intend to generate vegetation indices, such as the Normalized Difference Vegetation Index (NDVI), to assess the daily stress status of the plants. These indices will then be correlated with growth rate and gas exchange parameters to provide deeper insights into plant health and development in response to drought.

The envisioned utility of this robot spans three applications. Firstly, the robot's capability to offer a scalable, sensitive, and HTP approach for quantifying growth rate as a function of water availability allows the precise measurement of minor allele contributions to drought tolerance. This is relevant because of the polygenic nature of drought tolerance and the gradual accumulation of drought tolerance alleles that has to occur through many cycles of crossing, phenotyping, and selective breeding. Secondly, the platform serves as an invaluable tool for genetic mapping, which, in the case of polygenic traits, requires the utilization of large population sizes coupled with high levels of replication for the proper estimation of genetic values. Lastly, the application of this platform extends beyond assessing drought tolerance alone. It offers a versatile framework for examining plant responses to various stressors, such as simulated heatwaves (by increasing greenhouse temperature for brief intervals) and nutrient deficits and/or toxicities.

Root architecture: We have developed a methodology to visualize and measure grapevine roots using minirhizotrons. A minirhizotron is a flat box that allows a plant to grow while exposing its root system through a transparent wall for imaging and data collection. After several months of testing different materials and configurations, we developed a minirhizotron design measuring 12 x 16 x 1 inches, made of acrylic, at a cost of \$25-35 per box (Figure 12A). This design is simple to assemble and can be imaged using a standard flatbed scanner. We have also significantly improved our technique for growing plants in rhizotrons, ensuring that the “natural” root architecture is maintained during plant propagation and imaging. For image analysis, we developed a strategy that combines custom code and publicly available machine learning models for segmentation, such as SAM (Segment Anything Model) and RMBG v1.4 (Figure 12B). Once root masks are generated for each image, we extract several root architectural traits, including root size, vertical and horizontal size and distribution, root angle, root diameter, root color, and the number of roots, among others.

As a proof of concept, we used this technique to study 11 commercial rootstocks (101-14, 110R, 140Ru, 420A, 5C, Dog Ridge, Freedom, GRN3, Ramsey, Schwarzmann, and SO4) with 1 to 10 replications for each in our minirhizotrons over a 4-week period. We obtained images of each rhizotron every 2-3 days (Figure 12C).

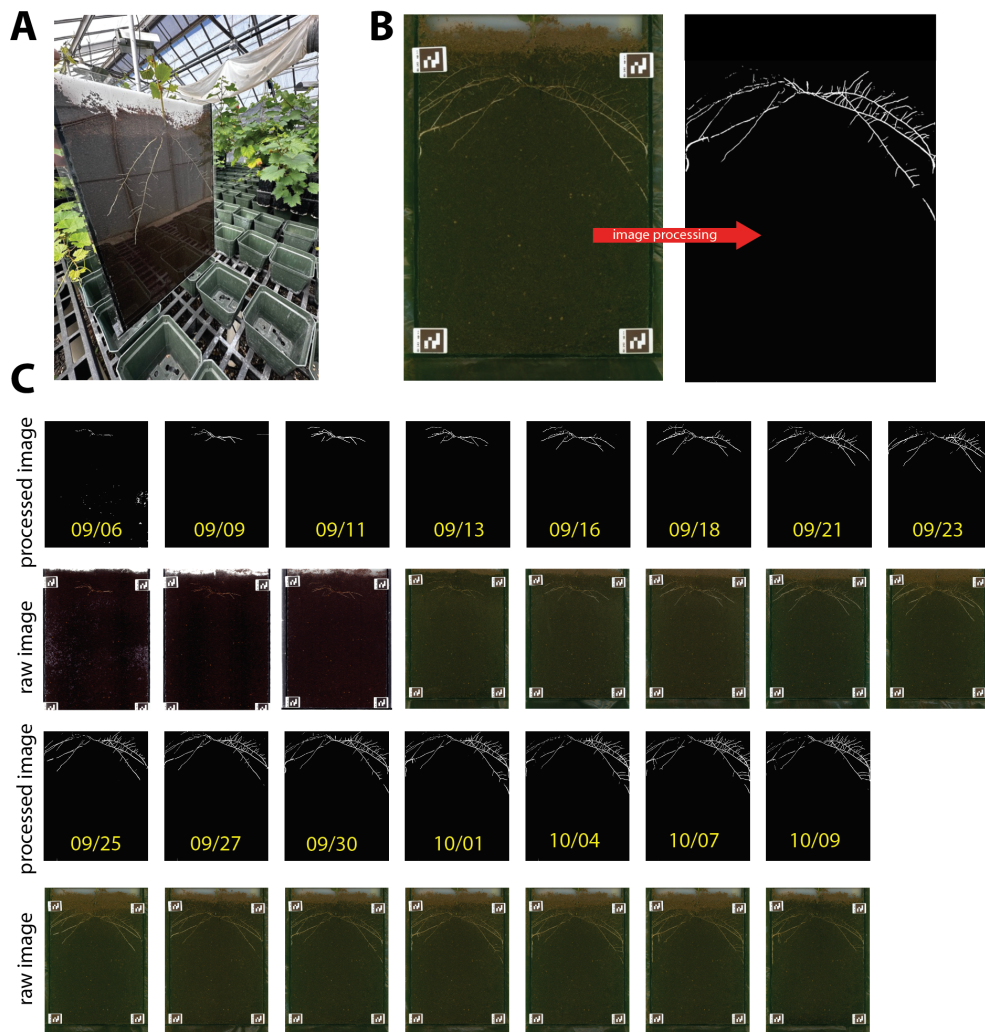


Figure 12. Minirhizotrons for root imaging. (A) Example of a rhizotron made of acrylic, measuring 12 x 16 x 1 inches, with rootstock Ramsey. (B) Image analysis showing the generation of root masks. (C) Timelapse of rootstock 5C, presented as both raw images and root masks.

We observed very large variability in root architecture across the genotypes studied. Root size, one of the simplest traits, varied by at least fourfold, with Ramsey having the largest root system (Figure 13A). Clear differences in spatial distribution were also observed. Ramsey exhibited a very deep root system, whereas 5C had an abundant but much shallower root distribution (Figure 13B). By combining multiple root architectural traits through Principal Component Analysis, sampling times (Figure 13C) and genotypes (Figure 13D) were clearly clustered. However, genotype clusters became more defined as the experiment progressed, with limited clustering at the beginning and stronger clustering toward the end.

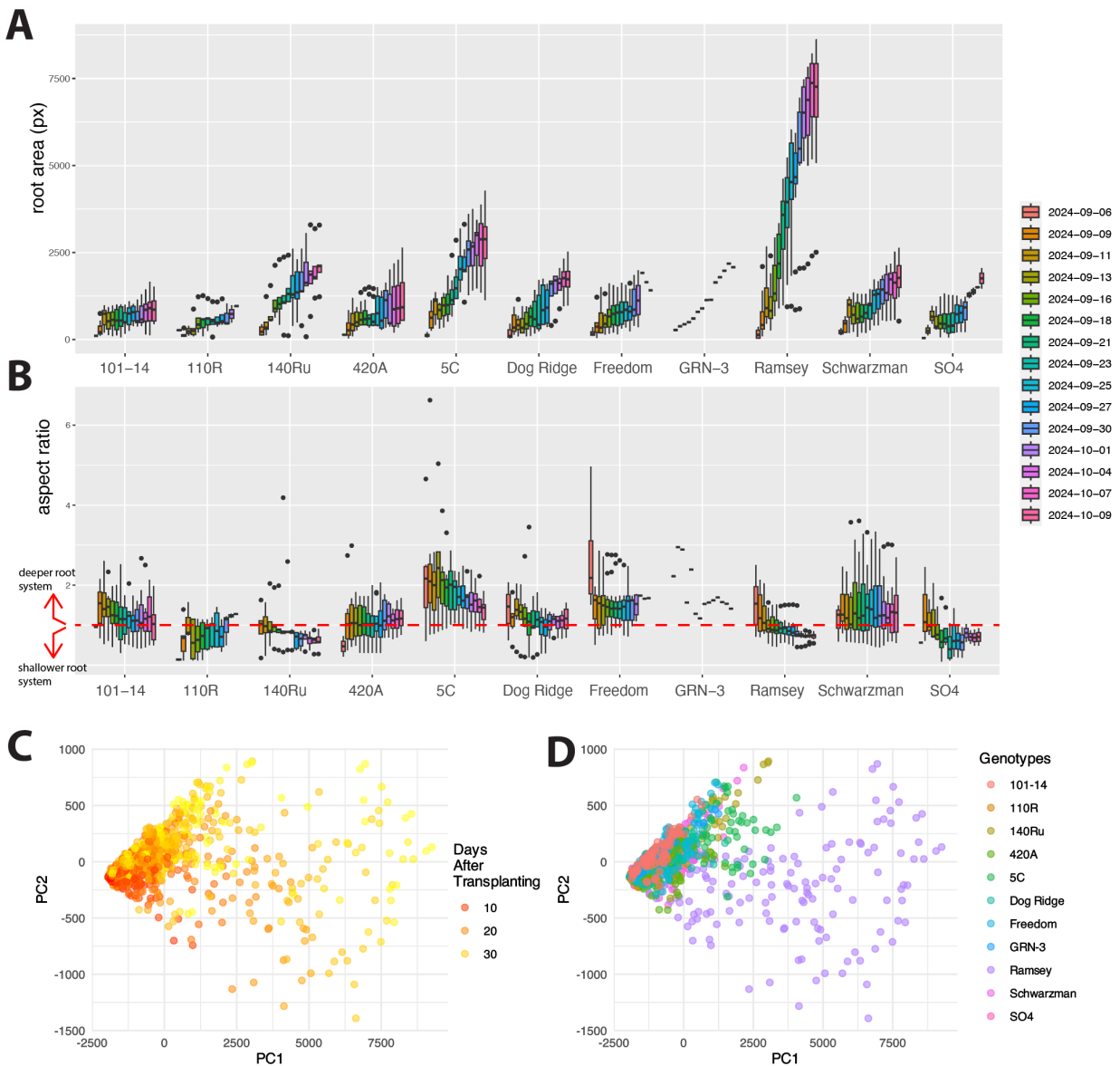


Figure 13. Root traits across time. (A) Root growth (total area, in pixels) and (B) aspect ratio across genotypes. Each boxplot represents between 1 (e.g., for GRN-3) and 10 repetitions (a repetition is a plant growing in its own rhizotron). Principal Component Analysis (PCA) was performed using root area, width, height, aspect ratio, perimeter, convex hull area, area per day, and depth gain per day. Markers are colored by (C) days after transplanting and (D) genotype.

This trial was intended to test our new methodology with a large number of rhizotrons, identifying potential issues and implementing fixes. It was not intended to fully characterize root architectures in commercial rootstocks. Over the next few months, we will conduct a larger trial to measure root architecture in the same rootstocks and additional ones, over a period of 4-6 weeks and under different irrigation regimes.

Following this, we will study a mapping population (n=120) derived from a cross between 101-14 and 110R, which segregates for root architecture. In collaboration with Megan Bartlett, we have genotyped this population and constructed genetic maps. Once the population is phenotyped using rhizotrons, we will conduct QTL mapping to identify molecular markers linked to root architectural traits.

Objective 3. Evaluate multi-species genomic and phenomic prediction models for faster cultivar development.

We continue to generate more: 1) plant material (primarily through crosses, but also some newly collected material), 2) phenotypic data (primarily from greenhouse trials), and 3) genotypic data (using genotyping-by-sequencing and rhAmpSeq markers). Within the next 2-5 years, we expect to have sufficient information to conduct genomic and phenomic predictions in grapevine rootstocks for traits such as drought and salinity tolerance (based on greenhouse trials), rooting ability (based on adventitious root formation), and field performance (yield, pruning weights, and phenology).

Other activities

Rooting ability: Adventitious root formation (ARF), the ability to form new roots post-embryonically from non-root tissues, varies significantly across *Vitis* species. Unfortunately, ARF is primarily skewed towards poor root formation in most *Vitis* species. *V. riparia* and *V. rupestris* are the only species with predominantly strong ARF and, therefore, constitute the foundation for most available rootstocks. ARF is essential for the cost-effective production of vines in nurseries, which limits the adoption of new rootstocks derived from non-conventional *Vitis* species outside the traditional trio. Many species and specific accessions with improved characteristics, such as the ones identified in the chloride and boron trials mentioned above, have poor ARF and are difficult to propagate via cuttings. Therefore, hybridization with *V. riparia*- or *V. rupestris*-based rootstocks is necessary.

We have assessed adventitious root formation in close to 200 accessions of 19 *Vitis* species. These accessions have been scored for ARF after callusing and 2 weeks after growth in soil. We are currently evaluating this phenotypic data, which we plan to integrate with genomic information in order to identify genetic variants linked to root formation.

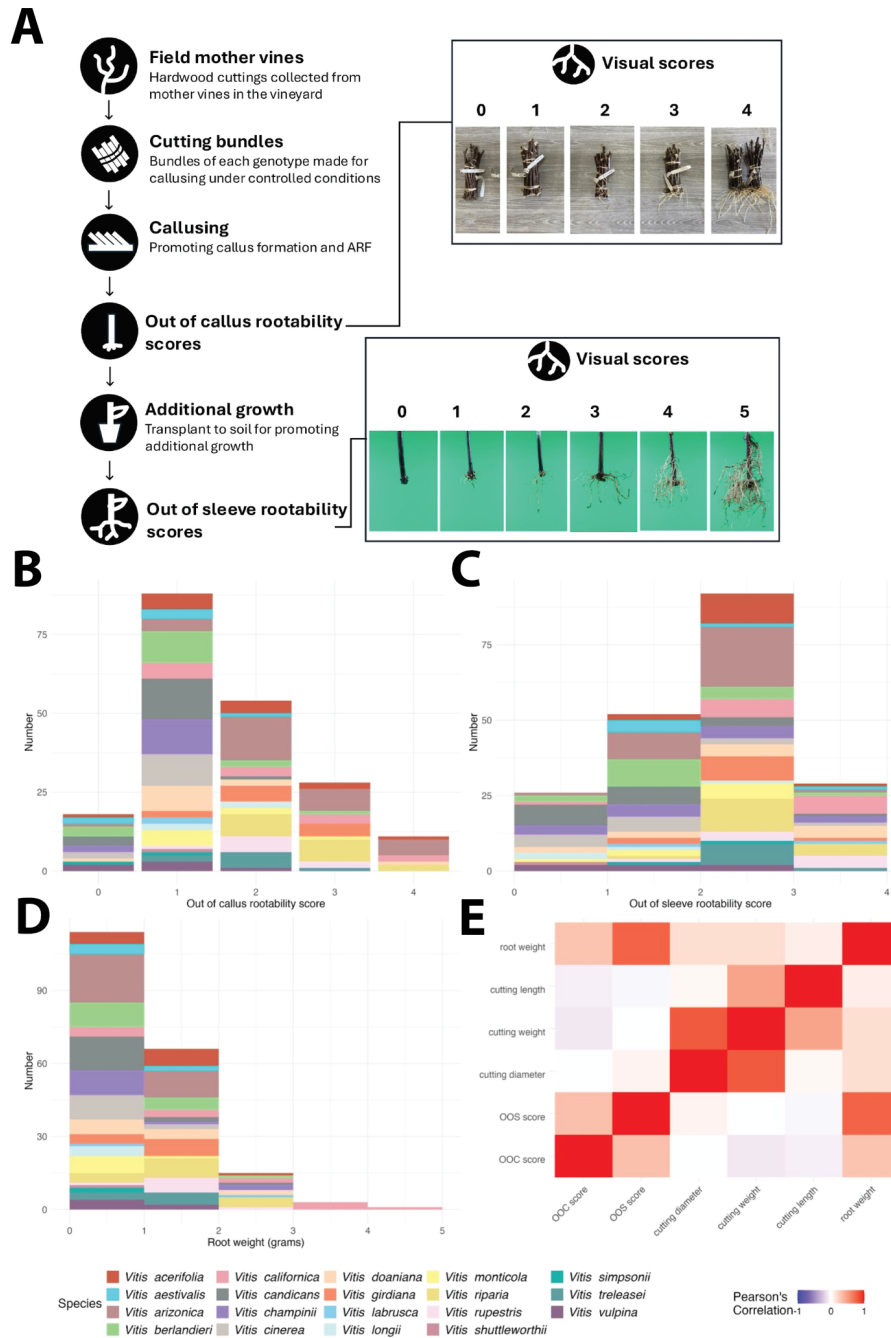


Figure 14. Rooting ability across *Vitis*. (A) Overview of the methodology used to assess rooting ability across *Vitis*. Rooting ability scores for grapevine cuttings range from 0 (no root formation) to 4 and 5 (extensive root formation) for “out of callusing” and “out of sleeve,” respectively. Distribution of (B) rooting scores for “out of callusing,” (C) rooting scores for “out of sleeve,” and (D) root weights. (E) Pearson’s correlation between ARF scores.

Posters/Abstracts at Scientific Meetings

1. Sharma, S., Diaz-Garcia, L. Non-Destructive Assessment of Chloride Content in Grape Leaves Using Spectroradiometer Opens Door for High-Throughput Phenotyping. 31 Plant and Animal Genome Conference. 12-17/01/24, San Diego, California
2. Sharma, S., Cochetel, N., Cantu, D., Diaz-Garcia, L. Genetics of adventitious root formation in dormant bud cuttings of grapevine. American Society for Horticultural Sciences Conference (ASHS). 24-27/09/2024, Honolulu, Hawaii.

Presentations to Industry Groups / Grower Advice

3. Diaz-Garcia, L. Rootstock breeding at UC Davis. CAMPOS (Center for the Advancement of Multicultural Perspectives on Science). 3/6/24, Davis, California
4. Diaz-Garcia, L. Foundations for a modern grape breeding program. 3rd Sustainable Viticulture Summit. 03/1/24, Online.
5. Lupo, Y. & Diaz-Garcia, L. Grapevine rootstocks' response to salinity. Emerging & Future Challenges in Viticulture. 04/17/24, Davis, California
6. Diaz-Garcia, L. Discussion panel, UC Davis Symposium on the Agricultural, Environmental and Social Sciences. 05/01/24, Davis, California
7. Diaz-Garcia, L. Overview of current breeding efforts at UCD. California Association of Winegrape Growers. 05/21/24, Davis, California
8. Diaz-Garcia, L. Grape breeding at UC Davis. Oakville Grape Day, 06/06/24. Oakville, California
9. Diaz-Garcia, L. Winegrape and rootstock breeding at UC Davis. Sustainable Ag Expo 11/13/24, San Luis Obispo, California
10. Diaz-Garcia, L. Retos que enfrentan los portainjertos en California. Cultivar – Farmworker Foundation. 11/15/24, Napa, California
11. Diaz-Garcia, L. Rootstock breeding efforts at UC Davis. 2024 Viticulture PT Meeting. 12/04/24, Davis, California.

Peer reviewed articles

12. Sharma, S., Wong, C., Bhattarai, K., Lupo, Y., Magney, T., & Diaz-Garcia, L. 2024. Hyperspectral sensing for high-throughput chloride detection in grapevines. *The Plant Phenome Journal*, 7, e70012. <https://doi.org/10.1002/ppj2.70012>

6. Funds Status

Most of the requested funds have been used to cover salaries and benefits for personnel involved in field and greenhouse experiments, as well as expenses for supplies, greenhouse space rental, vineyard pruning crews, and genotyping. The ongoing research activities for this project are currently funded by the California Grape Rootstock Improvement Commission and the California Grape Rootstock Research Foundation.